

Electronic structure and Fermi surface of new K intercalated iron selenide superconductor $K_xFe_2Se_2$

I.R. Shein, * A.L. Ivanovskii

*Institute of Solid State Chemistry, Ural Branch of the Russian Academy of Sciences,
620990, Ekaterinburg, Russia*

ABSTRACT

Using the *ab initio* FLAPW-GGA method we examine the electronic band structure, densities of states, and the Fermi surface topology for a very recently synthesized ThCr₂Si₂-type potassium intercalated iron selenide superconductor $K_xFe_2Se_2$. We found that the electronic state of the *stoichiometric* KFe_2Se_2 is far from that of the isostructural iron pnictide superconductors. Thus the main factor responsible for experimentally observed superconductivity for this material is the deficiency of potassium, *i.e.* the hole doping effect. On the other hand, based on the results obtained, we conclude that the tuning of the electronic system of the new $K_xFe_2Se_2$ superconductor in the presence of K vacancies is achieved by joint effect owing to structural relaxations and hole doping, where the structural factor is responsible for the modification of the band topology, whereas the doping level determines their filling.

PACS : 71.18.+y, 71.15.Mb, 74.25.Jb

Keywords: Superconducting $K_xFe_2Se_2$; electronic band structure; Fermi surface; hole doping effect; *ab initio* calculations

* Corresponding author.

E-mail address: shein@ihim.uran.ru

1. Introduction

Among the recently discovered [1] iron-based high-temperature superconductors (SCs) two main groups are found: so-called iron pnictide ($FePn$, where Pn are P, As, and Bi) and iron chalcogenide ($FeCh$, where Ch are S, Se, and Te) systems. For $FePn$ SCs, several structural families are known: ternary 111 (such as $LiFeAs$), 122 (such as $BaFe_2As_2$), quaternary 1111 (such as $LaFeAsO$), and five-component 32225 (such as $Sr_3Sc_2Fe_2As_2O_5$) and 42226 (such as $Sr_4V_2Fe_2As_2O_6$) systems. Their layered crystal structures include $[Fe_2Pn_2]$ building blocks alternating with planar sheets of alkaline or alkaline-earth metals (for 111 or 122 phases) or with more complex structural blocks (for 1111, 32225, and 42226 phases), reviews [2-9].

In turn, the $FeCh$ SCs form a family of simplest binary layered materials with blocks, in which Fe cations are tetrahedrally coordinated with Ch ions. These systems are known also as 11 phases. The transition temperatures T_C for these materials (for example, for $FeSe$) at ambient conditions are quite low and do not exceed 8K. Considerable efforts were undertaken recently to improve T_C of these binary 11 $FeCh$ phases: by partial substitutions of chalcogens ($S \leftrightarrow Se \leftrightarrow Te$), by substitutions of transition metals on the iron site, by external pressure etc., see reviews [10,11].

Very recently, two new unique ternary $FeCh$ SCs with enhanced T_C were discovered by intercalation of alkaline metal ions between $[Fe_2Se_2]$ blocks. Their nominal compositions are $K_{0.8}Fe_2Se_2$ [12] and $Cs_{0.8}Fe_2Se_{1.96}$ [13]. These phases possess the highest $T_C \sim 30K$ [12] and $T_C \sim 27 K$ [13] among all known $FeCh$ SCs under ambient pressure, see reviews [10,11]. Moreover, like the family of 122 $FePn$ materials, these phases adopt a tetragonal structure of the $ThCr_2Si_2$ type (space group $I/4mmm$).

According to [12,13], the enhanced superconductivity of the novel 122 $FeCh$ phases may be related to structural indicators, such as the so-called anion height (Δz , the distance of Pn (Ch) atoms from the Fe plane inside $[Fe_2Pn(Ch)_2]$

blocks) and Se-Fe-Se bond angles, which for these materials are closer to their "optimum" values ($\sim 1.38 \text{ \AA}$ and 109.47°) for iron based SCs, see [2,3,14]. The other key factor can be related to K(Cs) non-stoichiometry, which is responsible for the electronic concentration in the systems and therefore for the type of band filling. However, no data about the electronic properties of these novel 122 *FeCh* phases are hitherto available.

In view of these circumstances, in this Communication we present a detailed *ab initio* study of the recently discovered ThCr_2Si_2 -type KFe_2Se_2 and focus our attention on its electronic properties and the Fermi surface (FS) topology – as dependent on the above mentioned structural and electronic factors.

2. Models and computational aspects

According to [12], the new potassium intercalated iron selenide $\text{K}_x\text{Fe}_2\text{Se}_2$ adopts a tetragonal ThCr_2Si_2 -type structure (space group $I4/mmm$; #139). The atomic positions are K: $2a$ (0, 0, 0), Fe: $4d$ (0, $\frac{1}{2}$, $\frac{1}{4}$) and Se: $4e$ (0, 0, z_{Se}), where z_{Se} is the so-called internal coordinate. Further we shall examine this material with the nominal composition KFe_2Se_2 .

Firstly, we focused our attention on the electronic properties of KFe_2Se_2 as depending on the structural factors. For this purpose, full structural optimization of the stoichiometric KFe_2Se_2 was performed both over the lattice parameters and the atomic positions including the internal coordinate z_{Se} as no detailed atomic coordinates were known for this phase, and then the electronic properties of this phase were calculated. Next, similar calculations were continued using the experimental structural parameters [12] for the composition $\text{K}_{0.8}\text{Fe}_2\text{Se}_2$. For these two systems abbreviated further as KFS^{calc} and KFS^{exp} , their electronic band structures and FSs were obtained and analyzed.

Secondly, the effect of band filling on the electronic properties and the Fermi surface topology for $\text{K}_x\text{Fe}_2\text{Se}_2$ was considered. Here, using the rigid-band model, we removed $0.4e$, $0.3e$, and $0.2e$ from the KFS^{calc} and KFS^{exp} systems

and in this way simulated K-deficient compositions $K_x\text{Fe}_2\text{Se}_2$ with $x = 0.6, 0.7,$ and $0.8,$ respectively.

All our calculations were carried out by means of the full-potential method within mixed basis APW+lo (LAPW) implemented in the WIEN2k suite of programs [15]. The generalized gradient correction (GGA) to exchange-correlation potential in the PBE form [16] was used. The plane-wave expansion was taken to $R_{\text{MT}} \times K_{\text{MAX}}$ equal to 8, and the k sampling with $12 \times 12 \times 12$ k -points in the Brillouin zone was used. The hybridization effects were analyzed using the densities of states (DOSs), which were obtained by a modified tetrahedron method [17].

3. Results and discussion

The experimental [12] and calculated structural parameters for KFS^{exp} and KFS^{calc} are summarized in the Table 1. KFS^{calc} may be viewed as a “compressed” phase with reduced a and c parameters as compared with KFS^{exp} .

The calculated band structures, densities of states (DOSs), and Fermi surfaces for KFS^{exp} and KFS^{calc} are depicted in Figs. 1-3. For both systems, their electronic spectra are similar (see Fig. 1), namely (i) the Se $4p$ states occur between -6.5 eV and -3.5 eV with respect to the Fermi level ($E_{\text{F}} = 0$ eV); (ii) the bands between -2.4 eV and E_{F} are mainly of the Fe $3d$ character, and (iii) the contributions from the valence states of K to the occupied bands are very small. Thus, as with related 122 FePn phases [2-7], potassium atoms in KFe_2Se_2 are in the form of cations close to K^{1+} and provide charge transfer into conducting blocks $[\text{Fe}_2\text{Se}_2]^{n-}$.

Let us focus on the most important features of the electronic band structure, namely on the low-dispersive bands, which, for the family of 122 FePn materials, cross the Fermi level and are responsible for the features of the FS topology [2,3,9,18,19]. The examined KFe_2Se_2 phase has an increased number of valence electrons ($nve = 29$ e per formula unit) as compared with FeAs-based materials (for example, BaFe_2As_2 , where $nve = 28$ e per formula unit). This

leads to shifting of the Fermi level to the upper Fe d -like bands with higher k_z dispersion. As a result, both for KFS^{exp} and KFS^{calc} the above low-dispersive $d_{xy, xz+yz}$ bands are below E_F , Fig. 2.

It is well known that the Fermi surface of ThCr_2Si_2 -like 122 FePn SCs adopts a characteristic quasi-two-dimensional (2D) multiple sheet topology and consists of cylinder-like hole pockets along the Γ - Z direction and cylinder-like electron pockets along the X - P direction, see [2,3,9,18,19]. The above shift of the Fermi level leads to serious differences in the FSs for KFe_2Se_2 versus 122 FePn SCs (see Fig. 3): both for KFS^{exp} and KFS^{calc} the Fermi surfaces contain closed hole-like pockets centered at Z point - instead of cylinder-like sheets for 122 FePn materials.

On the other hand, we can see (Fig. 2) that for KFS^{exp} with increased lattice parameters the low-dispersive $d_{xy, xz+yz}$ bands come much nearer to E_F , and the closed hole-like pockets (around Z) are extended along the k_z direction acquiring a pronounced conical shape. Additionally this shift is accompanied by growth of total DOS at the Fermi level, $N(E_F)$, from 2.57 states/eV \cdot f.u. for KFS^{calc} up to 3.81 states/eV \cdot f.u. for KFS^{exp} , see Table 2. However based on the results obtained we find that the electronic state of the *stoichiometric* KFe_2Se_2 is far from those required for the iron-based high-temperature superconductors.

Thus, it may be concluded that the main factor responsible for the experimentally observed superconductivity for this material is the deficiency of potassium, *i.e.* the hole doping effect. Indeed, it is possible to explain this effect qualitatively using the band picture for the *stoichiometric* KFe_2Se_2 , Fig. 2. If K^{1+} ions are partially removed, the *nve* in the system lowers, high-dispersive Fe d -like bands get empty, and the Fermi level shifts to low-dispersive $d_{xy, xz+yz}$ bands forming an electronic picture typical of 122 FePn SCs.

To confirm this tendency, in Fig. 3 we present the Fermi surfaces for a set of potassium-deficient phases $\text{K}_x\text{Fe}_2\text{Se}_2$ for $x = 0.8, 0.7,$ and 0.6 as calculated in the framework of the above rigid-band model both for KFS^{exp} and KFS^{calc} systems.

As is seen, for KFS^{calc} , which keeps the optimized geometry for *stoichiometric* KFe_2Se_2 , at the first stage (from $x= 1.0$ to $x = 0.7$) the size of the closed Z-centered pocket decreases, and only at a high level of K deficiency ($x = 0.6$) a cylinder-like hole sheet arises.

On the contrary, for KFS^{exp} (with experimental lattice parameters for $\text{K}_{0.8}\text{Fe}_2\text{Se}_2$ phase) the cylinder-like sheet is formed already at $x = 0.8$, and further growth of K deficiency leads only to an increase in the diameter of this hole-like cylinder.

Thus, we conclude that the tuning of the electronic system of the new K intercalated iron selenide superconductor in the presence of potassium vacancies is achieved by joint effect owing to structural relaxations and hole doping. It is possible to assert that the structural factor is responsible for the modification of the band topology, whereas the doping level determines their filling.

4. Conclusions

In conclusion, we used the first-principle FLAPW-GGA approach to examine the band structure, density of states, and the Fermi surface topology for the recently synthesized ThCr_2Si_2 -type K intercalated iron selenide superconductor $\text{K}_x\text{Fe}_2\text{Se}_2$.

Our results show that the electronic state of the *stoichiometric* KFe_2Se_2 is far from that of isostructural iron pnictide superconductors, and the main factor responsible for experimentally observed superconductivity for this material is the deficiency of potassium, *i.e.* the hole doping effect. On the other hand, taking into consideration the results obtained, we conclude that the tuning of the electronic system of the new $\text{K}_x\text{Fe}_2\text{Se}_2$ superconductor in the presence of potassium vacancies is achieved by joint effect owing to structural relaxations and hole doping, where the structural factor is responsible for the modification of the band topology, whereas the doping level determines their filling.

Acknowledgments

Financial support from the RFBR (Grants 09-03-00946 and 10-03-96008) is gratefully acknowledged.

References

- [1] Y. Kamihara, T. Watanabe, M. Hirano, H. Hosono, *J. Am. Chem. Soc.* 30 (2008) 3296.
- [2] R. Pottgen, D. Johrendt, *Z. Naturforsch.* 63b (2008) 1135.
- [4] W. Jeitschko, B.I. Zimmer, R. Glaum, L. Boonk, U.C. Rodewald, *Z. Naturforsch.* 63b (2008) 934.
- [4] A.L. Ivanovskii, *Physics - Uspekhi* 51 (2008) 1229.
- [5] M.V. Sadovskii, *Physics - Uspekhi* 51 (2008) 120.
- [6] F. Ronning, E.D. Bauer, T. Park, N. Kurita, T. Klimczuk, R. Movshovich, A.S. Sefat, D. Mandrus, J.D. Thompson, *Physica C* 469 (2009) 396.
- [7] Z.A. Ren, Z.X. Zhao, *Adv. Mater.* 21 (2009) 4584.
- [8] M.D. Lumsden, A.D. Christianson, *J. Phys.: Cond. Matter* 22 (2010) 203203.
- [9] J.A. Wilson, *J. Phys.: Cond. Matter* 22 (2010) 203201.
- [10] M.K. Wu, F.C. Hsu, K.W. Yeh, T.W. Huang, J.Y. Luo, M.J. Wang, H.H. Chang, T.K. Chen, S.M. Rao, B.H. Mok, C.L. Chen, Y.L. Huang, C.T. Ke, P.M. Wu, A.M. Chang, C.T. Wu, T.P. Perng, *Physica C* 469 (2009) 340.
- [11] Y. Mizuguchi Y, Y. Takano, *J. Phys. Soc. Jpn* 79 (2010) 102001.
- [12] J. Guo, S. Jin, G. Wang, S. Wang, K. Zhu, T. Zhou, M. He, X. Chen, *Phys. Rev. B.* 82 (2010) 180520(R)
- [13] A. Krzton-Maziopa, Z. Shermadini, E. Pomjakushina, V. Pomjakushin, M. Bendele, A. Amato, R. Khasanov, H. Luetkens, K. Conder, 2010 *arXiv:1012.3637* (unpublished)
- [14] Y. Mizuguchi, Y. Hara, K. Deguchi, S. Tsuda, T. Yamaguchi, K. Takeda, H. Kotegawa, H. Tou, Y. Takano, *Supercond. Sci. Technol.* 23 (2010) 054013.
- [15]. P. Blaha, K. Schwarz, G.K.H. Madsen, D. Kvasnicka, J. Luitz, *WIEN2k, An Augmented Plane Wave Plus Local Orbitals Program for Calculating Crystal Properties*, (Vienna University of Technology, Vienna, 2001)
- [16] J.P. Perdew, S. Burke, M. Ernzerhof, *Phys. Rev. Lett.* 77 (1996) 3865.
- [17] P.E. Blochl, O. Jepsen, O.K. Anderson, *Phys. Rev. B* 49 (1994) 16223.
- [18] J. Fink, S. Thirupathaiah, R. Ovsyannikov, H.A. Dürr, R. Follath, Y. Huang, S. de Jong, M.S. Golden, Y.Z. Zhang, H.O. Jeschke, R. Valentí, C. Felser, S. Dastjani Farahani, M. Rotter, D. Johrendt, *Phys. Rev. B* 79 (2009) 155118.
- [19] W. Xie, M. Bao, Z. Zhao, B.G. Liu, *Phys. Rev. B* 79 (2009) 115128.

Table 1.

Structural parameters for KFe_2Se_2 : lattice constants (a , c , Å), internal coordinate (z_{Se}), bond length (d , Å), bond angles (Θ , °), and anion height (Δz , Å).

System * / parameter	KFS ^{calc}	KFS ^{exp} [12]
a	3.8608	3.9136
c	13.8369	14.0367
z_{Se}	0.3452	0.3539
$d(\text{K-Se})$	3.4700×8	3.4443×8
$d(\text{Fe-Se})$	2.3370×4	2.4406×4
$d(\text{Fe-Fe})$	2.7299×4	2.7673×4
Θ	111.41×4 ; 108.52×2	110.93×4 ; 106.60×2
Δz	1.3165	1.4237

* see text

Table 2.

Total and partial densities of states ($N(E_F)$, states/eV·f.u.) at the Fermi level for KFe_2Se_2 .

System / $N(E_F)$	KFS ^{calc}	KFS ^{exp}	System / $N(E_F)$	KFS ^{calc}	KFS ^{exp}
total	2.571	3.811	Fe $3d_{xz+yz}$	1.052	1.711
Fe $3d$	1.772	2.873	Se $4s$	0.008	0.011
Fe $3d_z^2$	0.023	0.032	Se $4p$	0.122	0.143
Fe $3d_{xy}$	0.631	1.058	Se $3d$	0.031	0.030
Fe $3d_{x^2-y^2}$	0.067	0.072			

FIGURES

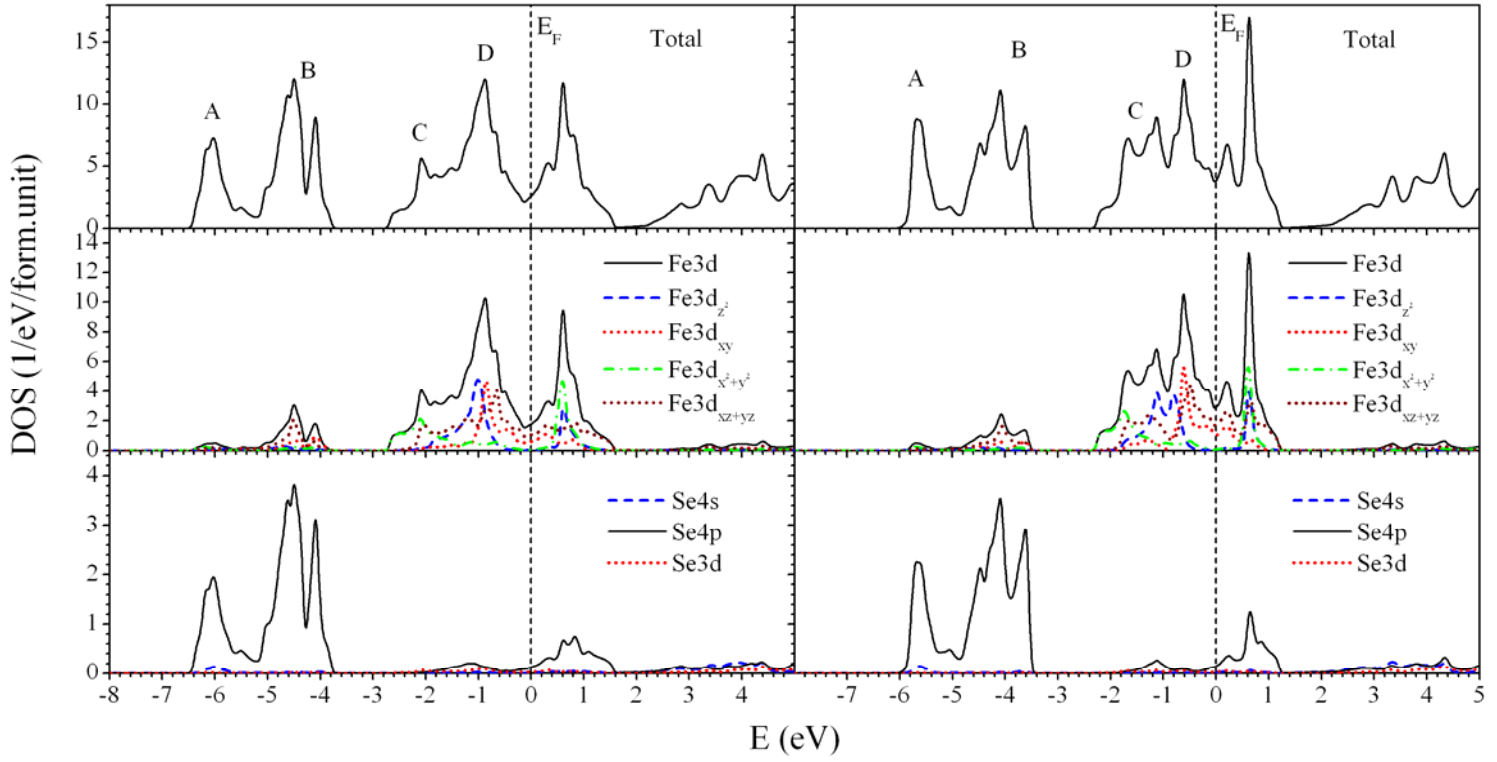


Fig. 1. Total (*upper panels*) and partial densities of states for KFS^{calc} (left), and for KFS^{exp} (right).

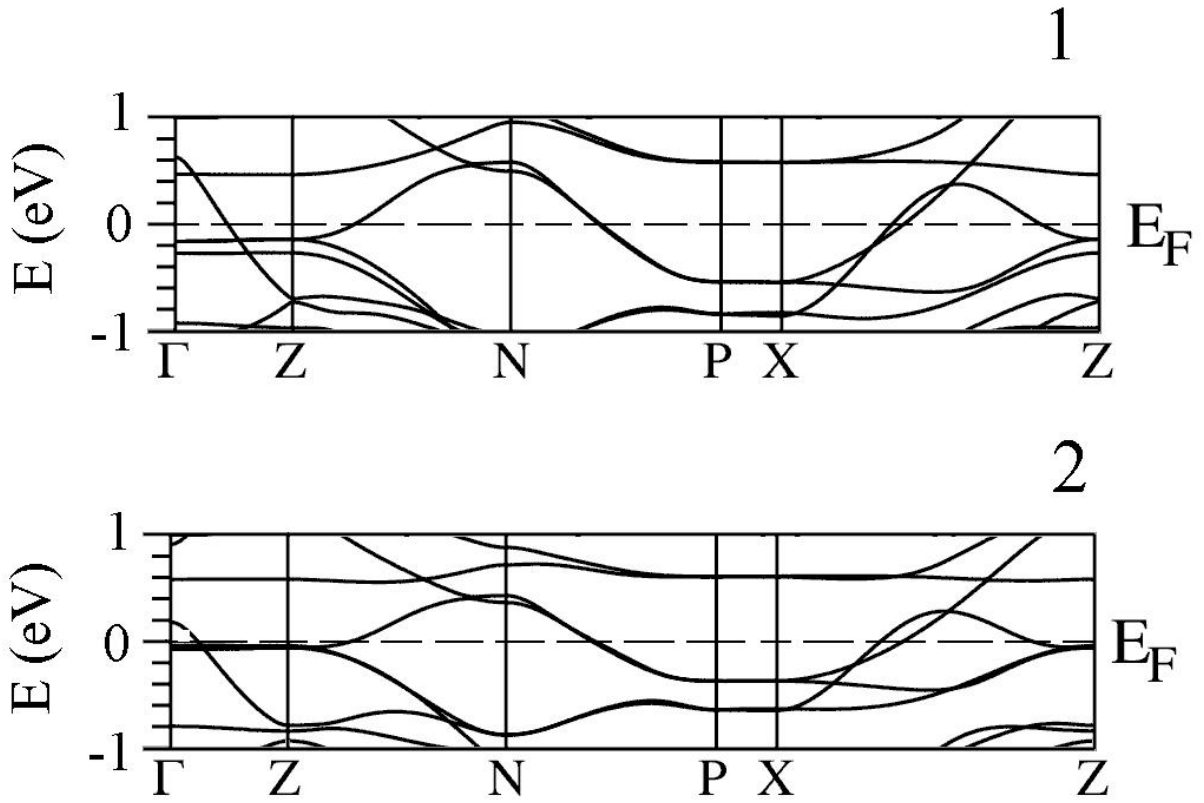


Fig. 2. Near-Fermi electronic bands for KFS^{calc} (1) and for KFS^{exp} (2).

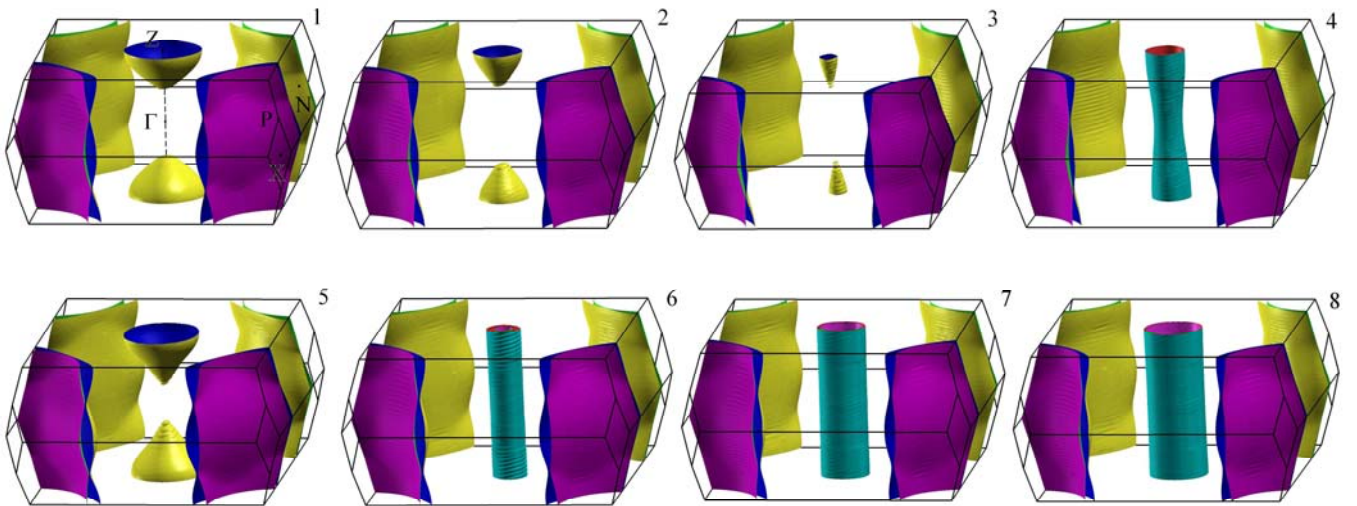


Fig. 3. Fermi surfaces for KFS^{calc} for $x = 1.0$ (1), 0.8 (2), 0.7 (3), and 0.6 (4) (*top panel*) and for KFS^{exp} for $x = 1.0$ (5), 0.8 (6), 0.7 (7), and 0.6 (8) (*bottom panel*).